JBC ACCELERATED COMMUNICATION

Structure of the second phosphoubiquitin–binding site in parkin

Received for publication, April 29, 2022, and in revised form, June 2, 2022 Published, Papers in Press, June 8, 2022,
https://doi.org/10.1016/j.jbc.2022.102114

Rayan Fakih, Véronique Sauvé, and Kalle Gehring*

From the Department of Biochemistry and Centre de recherche en biologie structurale, McGill University, Montreal, Quebec, Canada

Edited by George DeMartino

Parkin and PINK1 regulate a mitochondrial quality control system that is mutated in some early onset forms of Parkinson's disease. Parkin is an E3 ubiquitin ligase and regulated by the mitochondrial kinase PINK1 *via* a two-step cascade. PINK1 first phosphorylates ubiquitin, which binds a recruitment site on parkin to localize parkin to damaged mitochondria. In the second step, PINK1 phosphorylates parkin on its ubiquitin-like domain (Ubl), which binds a regulatory site to release ubiquitin ligase activity. Recently, an alternative feed-forward mechanism was identified that bypasses the need for parkin phosphorylation through the binding of a second phosphoubiquitin (pUb) molecule. Here, we report the structure of parkin activated through this feed-forward mechanism. The crystal structure of parkin with pUb bound to both the recruitment and regulatory sites reveals the molecular basis for differences in specificity and affinity of the two sites. We use isothermal titration calorimetry measurements to reveal cooperativity between the two binding sites and the role of linker residues for pUbl binding to the regulatory site. The observation of flexibility in the process of parkin activation offers hope for the future design of small molecules for the treatment of Parkinson's disease.

Parkinson's disease (PD) is the second most common neurodegenerative disease. It is characterized by motor symptoms due to the progressive loss of dopaminergic neurons of the *substantia nigra* in the midbrain. While most PD cases are sporadic and occur later in life, 5% to 10% of cases are inherited through autosomal mutations, which induce early onset of the disease (1). Many of these mutations are found in the *PARK2* and *PARK6* genes, which encode for the parkin and PTEN-induced putative kinase protein 1 (PINK1), respectively (2, 3). Parkin and PINK1 are involved in mitochondrial quality control, wherein damaged mitochondria are targeted for autophagy through the polyubiquitination of proteins on the outer mitochondrial membrane (4). Parkin and PINK1 also mediate autophagy-independent processes, such as the formation of mitochondrial-derived vesicles to excise damaged mitochondrial portions and the suppression of mitochondrial antigen presentations (5, 6).

Parkin is a cytosolic E3 ubiquitin ligase consisting of an N-terminal ubiquitin-like domain (Ubl) linked to a R0RBR module formed by four zinc-coordinating domains, a unique RING0 domain and three other zinc-finger domains (RING1, IBR, and RING2), which are characteristic of the ring-between-ring (RBR) family of E3-ubiquitin ligases. Typical of RBR-type E3 ligases, parkin uses a RING/HECT hybrid mechanism, wherein RING1 behaves as a scaffold and binds ubiquitin-charged E2 enzymes, and RING2 forms a thioester intermediate with incoming ubiquitin molecules through a reactive cysteine (7). Early crystal structures of parkin reveal that it adopts an autoinhibited conformation under basal conditions. The RING1 E2-binding site is obstructed by the Ubl domain and a repressive alpha helical linker (REP) located between IBR and RING2 domains, and the RING2 reactive cysteine is occluded by interactions with the RING0 domain (8–10).

To mediate the transfer of ubiquitin onto damaged mitochondrial proteins, parkin must translocate to the mitochondria and undergo a conformational change to release its autoinhibition. Both events depend on PINK1, a mitochondrial serine/threonine kinase, which behaves as a sensor for mitochondrial defects (11–14). Following mitochondrial damage, PINK1 accumulates on the surface of the mitochondria and phosphorylates nearby ubiquitin molecules at serine 65. Parkin binds to the phosphorylated ubiquitin (pUb) with high affinity through its RING1 domain and accumulates on the mitochondria (15–20). Parkin is then phosphorylated on its Ubl domain by PINK1 and undergoes structural rearrangement, activating its ubiquitin ligase function (17, 21–25). Recent crystal structures of the complex of phosphorylated parkin with pUb reveal that the phosphorylation of Ubl (pUbl) on its serine 65 residue is responsible for conformational changes within parkin leading to its activation (26, 27). Phosphoserine (pS65) of pUbl binds a phosphate-binding pocket located on RING0 domain near the RING0–RING2 interface. The binding of pUbl onto RING0 then displaces the catalytic RING2 domain. The structure of activated parkin also reveals that a segment of the linker between the Ubl and RING0 domains, named the activation (ACT) element, makes additional contacts between RING0 and Ubl at a position previously occupied by RING2 and REP (27). The release of RING2 from RING0 exposes the reactive cysteine and allows the

* For correspondence: Kalle Gehring, kalle.gehring@mcgill.ca.

subsequent transfer of ubiquitin molecules from ubiquitin-charged E2 enzymes onto target proteins. The newly added ubiquitin chains on the mitochondrial outer membrane provide more substrates for PINK1 (28). This leads to further recruitment of parkin molecules to the mitochondria, thereby amplifying the signal for autophagy through a positive feedback mechanism (20, 29, 30).

Parkin is also involved in an open-cycle or feed-forward mechanism that does not depend on parkin phosphorylation (31). We recently showed that binding of pUb to the RING0 pUbl-binding site can mediate phosphorylation-independent activation of parkin. This explains the previous observations that removal or mutation of the Ubl domain does not completely abolish its recruitment to the mitochondria or parkin-mediated mitophagy in cells (20, 32–34). In the feed-forward mechanism, pUb functions both as a signal for parkin recruitment and activation.

Here, we use analytical ultracentrifugation to confirm that parkin can bind two pUb molecules and isothermal titration calorimetry experiments to characterize cooperativity and the role of the Ubl-RING0 linker in pUbl binding. We use X-ray crystallography to reveal the structural features responsible for the specificity and selectivity of the pUb-binding sites. The work offers perspectives on the possible existence of alternative activation pathways of parkin in cells and the development of small molecules to affect its activation in PD.

Results

Parkin has two binding sites for phosphorylated ubiquitin

We used analytical ultracentrifugation to confirm that parkin has two binding sites for pUb (Table 1). A minimal parkin construct consisting only of the RING0, RING1, and IBR domains (termed R0RB) was generated. This fragment contains the two phosphoserine-binding sites but not the catalytic domain that competes for binding to the RING0 site. Sedimentation velocity experiments with the R0RB fragment measured a single species with an inferred molecular mass of 26.5 kDa (Fig. S1). Addition of one equivalent of pUb increased the apparent mass by 9.5 kDa in agreement with the predicted molecular mass. Addition of ten equivalents led to two sedimenting species, one at 43.7 kDa as expected for R0RB with two pUb bound and a second species corresponding to free pUb. All three analyses showed residuals of less than ± 0.01 absorbance units with a single peak for R0RB in the c(s) size-distribution analysis.

Structure of parkin with pUb bound to RING0

We used protein crystallography to determine the structure of the R0RB fragment of parkin with two pUb molecules bound. Crystals were obtained by vapor diffusion in the presence of 0.1 M Bis–Tris propane pH 7.5, 0.1 M NaI, and 20.5% PEG3350. The crystals diffracted to 2.48 Å and were solved by molecular replacement using the structure of human phosphorylated parkin (Table S1).

The structure shows pUb molecules bound to the RING1 and RING0 phosphoserine-binding sites (Fig. 1*A*). The structure is similar to previous structures of activated parkin but with pUb replacing pUbl on RING0 (26, 27) (Fig. 1, *B* and *C*). Overlaying of the pUb and pUbl in the two structures shows the largest conformational shifts are in the loop formed by residues 7 to 11, in agreement with previous modeling (31) (Fig. 1*D*). The alpha-carbon of threonine 10 in pUb is shifted by over 4 Å from the corresponding serine in pUbl (parkin). This loop is also the site of the largest conformational differences between pUb bound to the RING1 and RING0 sites. In contrast, the RING0 domain shows only small shifts in the alpha-carbon positions between the pUbl- and pUb-bound structures.

Binding of pUb (and pUbl) to RING0 is principally mediated by phosphoserine binding to the positively charged pocket formed by lysine (K161), arginine (R163), and lysine (K211) (Fig. 1, *E* and *F*). Key hydrophobic interactions further contribute to binding, notably, isoleucine (I44) and valine (V70) on β3 and β4 and a loop containing a conserved glycine (G47), which inserts into the hydrophobic groove of RING0 (Fig. 1, *G* and *H*). The shift in residues 7 to 11 allows pUb to form an additional hydrophobic contact between pUb leucine (L8) and RING0 proline (P199). In pUbl, this leucine is asparagine (N8) and the loop faces away from RING0 (Fig. 1, *G* and *H*). Overall, pUb forms more direct contacts with RING0 than pUbl, which leads to its roughly threefold higher affinity in isothermal titration calorimetry (ITC) experiments (31).

Specificity of the RING1 pUb-binding site

In hindsight, it is not surprising that pUb binds to the RING0-binding site. Ubiquitin and the parkin Ubl domain share 30% identity and 29% conservative substitutions (Fig. 1*C*). They are phosphorylated on the same serine residue and have the same hydrophobic patch centered around isoleucine 44 (Fig. 1*C*). Rather, it is the inability of pUbl to bind the RING1 site that is the more remarkable feature that requires explanation. Strong selectivity elements must exist to prevent the intramolecular binding of the pUbl, which, as an intramolecular ligand, is present at a high local concentration in phosphorylated parkin. Binding of pUb to RING1 is an essential step in the PINK1–parkin pathway; mutations in the RING1-binding site cause early onset PD (35–37). pUbl

Table 1
Ultracentrifugation analysis of parkin R0RB–pUb complexes

R0RB (μM)	pUb (μM)	Sedimentation coefficient (S)	Experimental MW (kDa)	RMSD	Theoretical MW (kDa)
10	0	2.43	26.5	0.0036	26.9
10	10	3.05	36.0	0.0029	35.4
10	100[a]	3.22	43.7	0.0028	44.0

Abbreviation: MW, molecular weight.
[a] A second peak from unbound pUb was observed at 1.20 S.

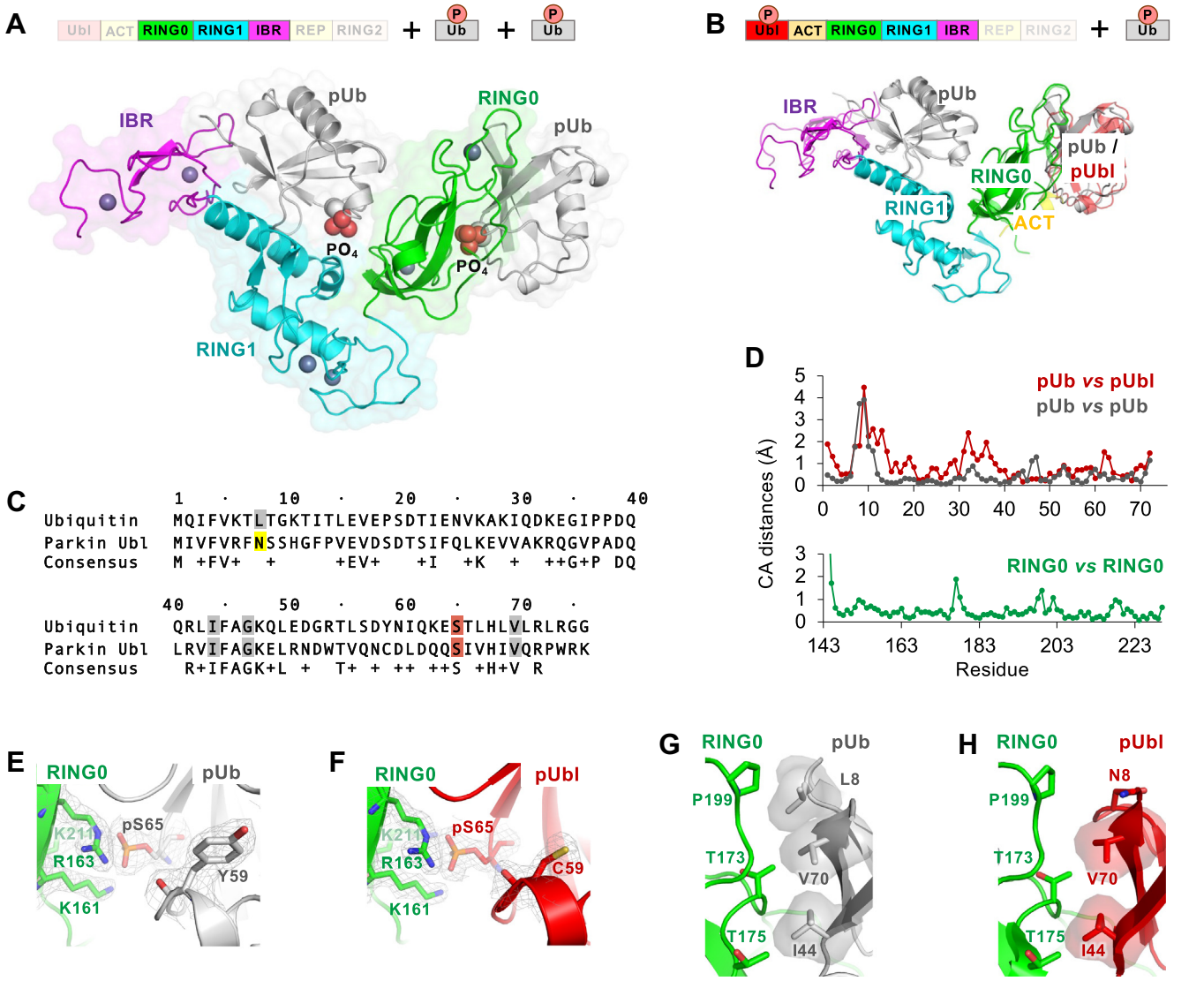

Figure 1. Structure of the parkin–2 × pUb ternary complex. *A*, domain organization and crystal structure of the parkin R0RB domains bound to two pUb molecules (R0RB–2 × pUb). *B*, comparison with structure of pUbl-R0RB–pUb (PDB 6GLC). *C*, alignment of amino acid sequences of ubiquitin and human parkin (Ubl). The serine 65 phosphorylation site, asparagine 8, and residues comprising the hydrophobic surface are highlighted. *D*, shifts in α-carbon positions for overlays of pUb and pUbl bound to RING0 (*red*), pUb bound to RING1 and RING0 (*gray*), and RING0 in the two structures (*green*). *E* and *F*, comparison of the RING0 phosphoserine-binding sites. The electron densities in the $2F_O$-F_C maps for tyrosine (Y59) in pUb and cysteine (C59) in pUbl confirm the identities of the polypeptide chains. *G* and *H*, comparison of the hydrophobic interactions. Leucine (L8) in pUb enlarges the interaction surface, interacting with RING0 proline (P199). PDB, Protein Data Bank; pUb, phosphorylated ubiquitin; Ubl, ubiquitin-like domain.

binding to RING1 would prevent both parkin recruitment to mitochondria and its activation. In addition to maintaining selectivity, the RING1 domain has to bind pUb with nanomolar affinity to efficiently recruit parkin to mitochondria. In ITC experiments, the RING1 domain displays one to two orders of magnitude higher affinity than RING0 for binding pUb (31).

To gain insight into the selectivity, we overlaid pUbl on pUb bound to RING1 (Fig. 2). The majority of molecular interactions match: phosphoserine (pS65) fits into the phosphate-binding cavity and the hydrophobic interactions are largely conserved. Unlike RING0, which binds pUb or pUbl without contacts from adjacent domains (Fig. 1*B*), Ub on RING1 makes multiple contacts with the neighboring RING0 and IBR domains (Fig. 2, *A* and *B*). This enlarged contact surface likely contributes to the higher affinity of the RING1 site. Comparing pUb and pUbl, the major differences are electrostatic and differences around the variable residue 7 to 11 loop. Substitution of asparagine (N60), glutamine (Q62), and lysine (K63) in pUb by two aspartic acids and a glutamine in pUbl results in a net change of three negative charges at the binding interface (Fig. 2, *A* and *C*). This would lead to electrostatic repulsion by glutamic acid (E300) on RING1. The pUbl hydrophobic binding surface is also smaller as observed at the RING0-binding site (Fig. 1, *G* and *H*). Substitution of leucine (L8) by asparagine in pUbl removes the hydrophobic contacts with the IBR and RING1 domains (Fig. 2, *B* and *D*). The shortening or lack of other hydrophobic residues in Ubl (serine 9, valine 36, and proline 73) may further contribute to the inability of pUbl to bind RING1 (Fig. 1*C*).

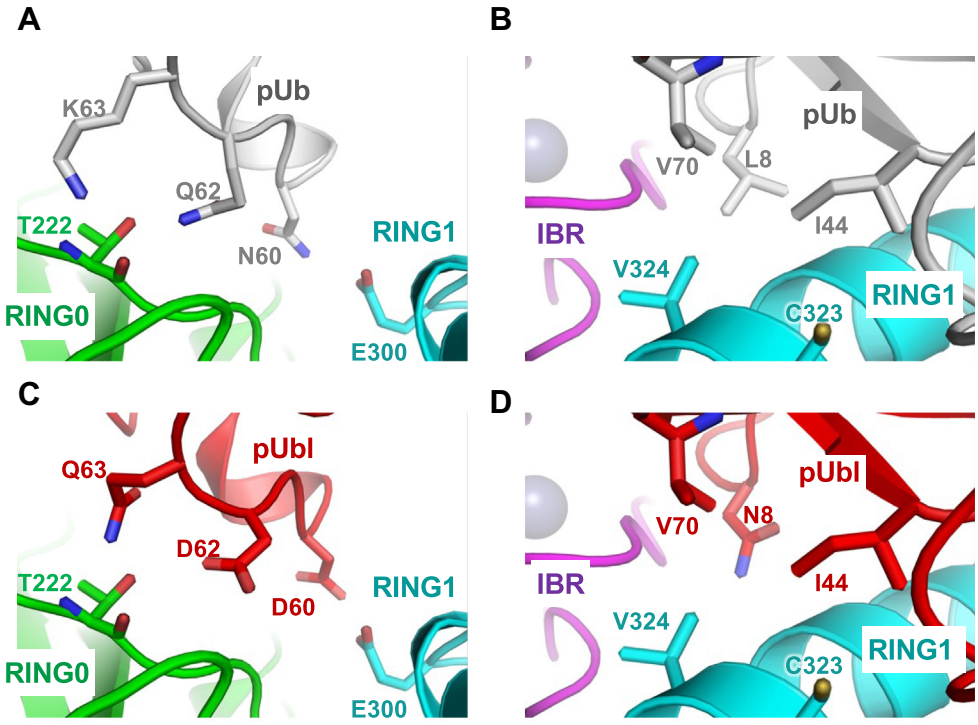

Figure 2. Specificity of RING1 pUb-binding site. Comparison of pUb bound to RING1 (*A* and *B*) with a hypothetical model with pUbl bound (*C* and *D*). Substitutions of asparagine (N60), glutamine (Q62), and lysine (K63) in ubiquitin (*A*) by negatively charged or neutral residues in parkin (*B*) leads to electrostatic repulsion, preventing pUbl binding. Substitution of leucine (L8) by asparagine (N8) disrupts the hydrophobic interactions with RING1 and IBR domains (*B* and *D*) further contributing to the specificity for pUb. pUb, phosphorylated ubiquitin.

The ACT element improves pUbl binding to RING0

In studies of the conformation of activated human parkin, several residues in the linker between Ubl and RING0 domains were observed to bind a hydrophobic patch on RING0 (27). Termed the ACT element, the linker was proposed to contribute to RING2 release and parkin activation. To test this, we used ITC experiments to quantify the contribution of the ACT element to pUbl binding to RING0 (Fig. 3). As we previously reported (31), titration of R0RB with pUbl measured a binding affinity of 1.1 μM (Fig. 3*A*). When the titration was repeated with a longer construct that includes the ACT element (pUbl-ACT), the affinity improved threefold (Fig. 3*C*). The ACT element also improved the affinity when binding was measured in the presence of a single equivalent of pUb (R0RB:pUb) (Fig. 3, *B* and *D*). In agreement with these results, our crystal structure showed residues from an N-terminal cloning artifact bound to the same hydrophobic patch on RING0 (Fig. S2). Following cleavage of the glutathione-*S*-transferase (GST)-affinity tag, our R0RB parkin construct contains five residues, GPLGS, from the 3C protease cleavage site. The electron density map revealed the GPLGS extension adopts two conformations with the proline and leucine residues inserted into the hydrophobic groove occupied by the ACT element in the structure of activated human parkin (pUbl-R0RB:pUb).

The binding studies additionally detected positive cooperativity between the RING1- and RING0-binding sites (Fig. 3). Comparison of pUbl (or pUbl-ACT) binding in the absence or presence of pUb revealed a 30% to 40% improvement in affinity when pUb was present. Although relatively small, the cooperativity contributes to the tight coupling of parkin localization and activation on the surface of damaged mitochondria. Parkin is more easily activated when bound to pUb and, conversely, once activated parkin is less likely to dissociate from the mitochondrial membrane.

Discussion

The regulation of mitochondrial quality control by parkin requires two steps controlled by the PINK1 kinase: parkin translocation to the mitochondria and activation of its ligase activity. PINK1 phosphorylates ubiquitin molecules on the surface of damaged mitochondria, which bind the RING1 domain on parkin with high affinity and effectively recruit the ligase to the mitochondrial surface (15–20). Canonically, parkin is then phosphorylated by PINK1 on its Ubl domain, which then binds the RING0 domain to release the catalytic RING2 domain (17, 21–24, 26, 27). We recently showed that an alternative mechanism exists where the autoinhibition on parkin can be released without its phosphorylation (31). In the feed-forward pathway, a second pUb molecule replaces the parkin pUbl domain and binds RING0 to allosterically activate parkin.

The three-dimensional structure of pUb binds to RING0, which is a compelling evidence for the existence of the feed-forward pathway but its importance in PD is unclear. The Ubl domain is conserved across evolution, and multiple disease mutations (R42P, V56E) occur in the domain (38, 39). While this would suggest that the feed-forward pathway is not

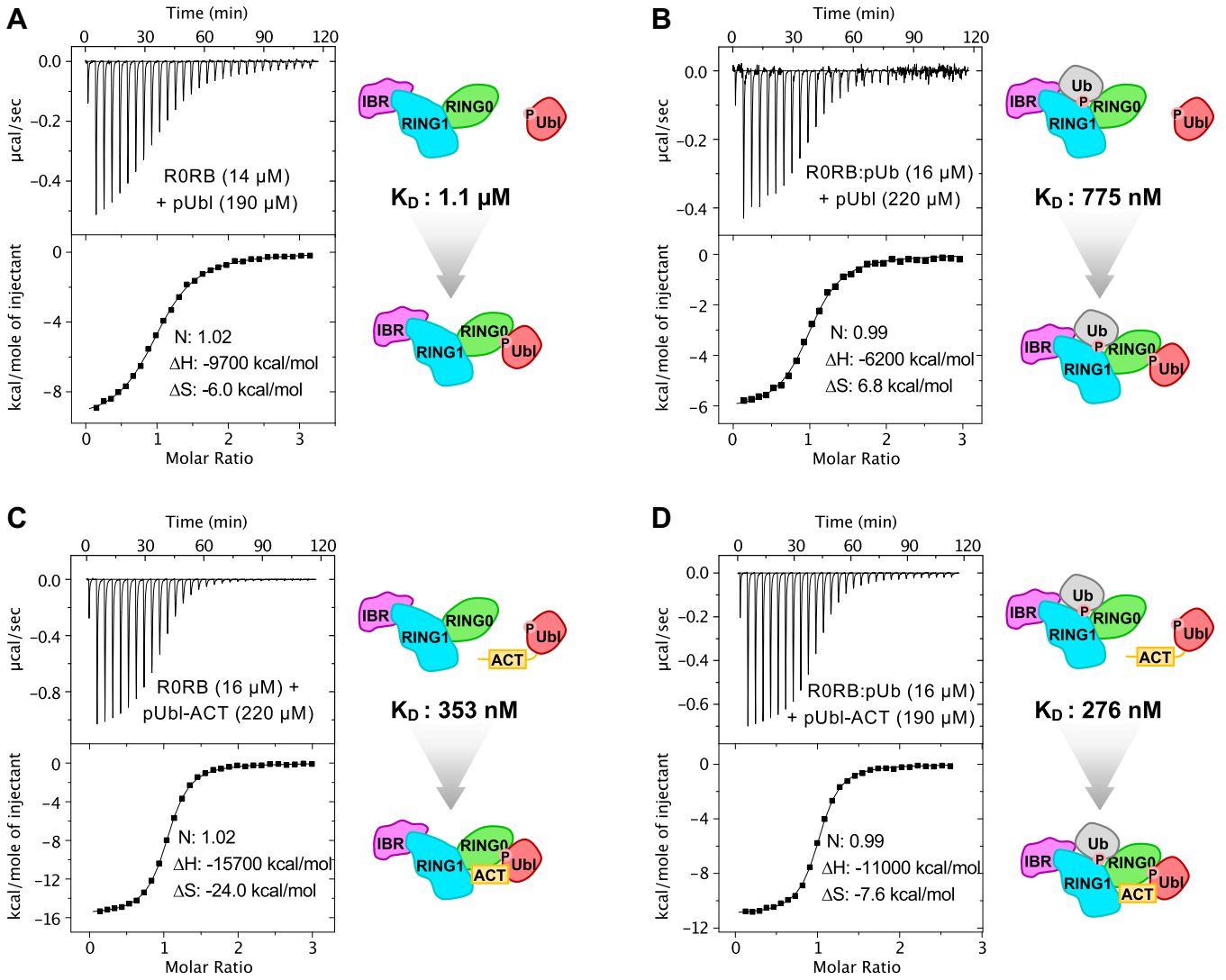

Figure 3. Secondary contributions to affinity of RING0 site. Isothermal titration calorimetry thermograms of (*A*) pUbl binding R0RB, (*B*) pUbl binding the complex of R0BR and pUb, (*C*) pUbl-ACT binding R0RB, (*D*) pUbl-ACT binding the complex of R0BR and pUb. pUb bound to the RING1 site increases the affinity of RING0 site by 1.4-fold; inclusion of the ACT linker sequence increases it threefold. ACT, activation; pUb, phosphorylated ubiquitin.

sufficient to prevent disease, the mutations also decrease the levels of parkin expression, which could be responsible for their disease association (35, 40). When the canonical pathway is inactivated in cultured cells, the feed-forward pathway rescues roughly a quarter of mitophagy as measured by mt-Keima assays (31). How this translates into parkin function in neurons is unknown.

Surprisingly, ITC measurements with the isolated domains show that pUb has higher intrinsic affinity for RING0 than the pUbl domain (31). In intact parkin, two factors increase the binding of the pUbl domain. The first is the ACT element, which increases the binding affinity of the pUbl domain, making it equal to pUb when measured *in trans*. The second is that pUbl binds as an intramolecular ligand with a local concentration, estimated to be in the millimolar range. These explain the dominance of parkin phosphorylation as the activation mechanism in cellular models.

The structure of pUb bound to RING0 raises possibility of other alternative activation mechanisms. Molecular recognition by RING0 is unexpectedly plastic; other phosphoproteins could bind to the pUbl-binding site to liberate parkin ligase activity. Parkin was shown to be recruited to synaptosome membranes from the mouse brain in a phosphorylation-dependent manner by an unknown factor (41). More recently, the ubiquitin-like protein NEDD8 was reported to be phosphorylated on serine 65 by PINK1 and to activate parkin (42). NEDD8 was also suggested to bind the pUb-binding site of RING1 as an alternative mechanism for parkin recruitment (43). These discoveries reveal unexplored complexity in parkin/PINK1 signaling and offer hope of novel avenues for the treatment of PD.

Experimental procedures

Cloning, expression, and purification of recombinant proteins

Rattus norvegicus parkin R0RB constructs (res. 141–379 and 145–379), Ubl (res. 1–76), and Ubl-ACT (res. 1–110) were subcloned into the BamHI-XhoI sites pGEX-6P-1

(GE Healthcare) with an N-terminal GST tag. A pRSF-Duet1–derived construct previously used to coexpress untagged *Tribolium castaneum* PINK1 (res. 121–570) and ubiquitin (26) was modified using the QuikChange Lightning Site-Directed Mutagenesis Kit (Agilent) to delete glycine 76 in ubiquitin. For crystallization, pGEX-6P-1 R0RB (res. 145–379) and pRSF-Duet1-PINK1-UbΔG76 were cotransformed into BL21 (DE3) *Escherichia coli* for the coexpression of the three proteins. For ITC assays, R0RB (res. 141–379), Ubl, and Ubl-ACT were expressed separately.

Protein expression of rat parkin R0RB, R0RB–pUb complexes, Ubl, and Ubl-ACT were performed as described previously (31). In brief, proteins were purified by glutathione-Sepharose (Cytiva) affinity chromatography, followed by overnight 3C protease cleavage to remove the GST tag. R0RB–pUb complex for crystallization was further purified by size-exclusion chromatography in 30 mM Tris pH 8.0, 150 mM NaCl, 1 mM tris(2-carboxyethyl)phosphine (TCEP). For ITC assays, proteins were subjected to size-exclusion chromatography in 50 mM Tris, 150 mM NaCl, 1 mM TCEP, pH 7.4 (ITC buffer). Purified proteins were verified by SDS-PAGE analysis. Protein concentrations were determined using UV absorbance.

Phosphorylation of Ub, Ubl, and Ubl-ACT

Hundred micromolar of commercial bovine ubiquitin (Sigma), rat Ubl, or rat Ubl-ACT was phosphorylated using 3 μM PINK1 in 50 mM Tris pH 7.4, 150 mM NaCl, 5 mM ATP, and 10 mM $MgCl_2$ at 30 °C for 2 h. Phosphoubiquitin was purified following a previously reported method and buffer exchanged in ITC buffer (24). Phospho-Ubl and phospho-Ubl-ACT were further purified by size exclusion in ITC buffer.

Sedimentation-velocity analytical ultracentrifugation

Sedimentation velocity analytical ultracentrifugation experiments were performed at 20 °C using a Beckman Coulter XL-I analytical ultracentrifuge using an An-60Ti rotor at 98,000*g* (35,000 rpm) for 18 h with scans performed every 60 s. A double-sector cell, equipped with a 12 mm Epon centerpiece and sapphire windows, was loaded with 380 and 400 μl of sample and buffer (30 mM Tris pH 8.0, 150 mM NaCl, 1 mM TCEP), respectively. Ten micromolar of R0RB supplemented with 0 to 10 equivalents of pUb was monitored with UV at 280 nm. The data was analyzed with Sedfit version 1501b (https://spsrch.cit.nih.gov/default.aspx) using a continuous c(s) distribution (44). Numerical values for the solvent density and viscosity were calculated to be 1.0053 g/cm^3 and 0.01020 mPa·s, respectively, using Sednterp. Partial specific volumes were defaulted to 0.73 cm^3/g, and the frictional ratio (f/f_0) values were floated. Residual and c(s) distribution graphs were plotted using GUSSI (45).

Crystallization

Crystals of the R0RB–2 × pUb complex were grown at 4 °C using sitting-drop vapor-diffusion by mixing 1 μl of protein complex (15–25 mg/ml) with 1 μl of 20.5% (w/v) PEG3350, 0.1 M NaI, 0.1 M Bis–Tris propane, pH 7.5. Crystals appeared within 1 to 2 days. After a week, crystals were cryoprotected in mother liquor supplemented with 25% (v/v) ethylene glycol before being flash frozen in liquid nitrogen.

Data collection and structure determination

Diffraction data for the complex was collected at the CMCF beamline 08B1-1 at the Canadian Light Source. A total of 360 images were collected with an oscillation angle of 0.5° at 1.1808 Å. Reflections were integrated and scaled with the MxLive platform (46) and then with the XDS package (47). The structure was solved by molecular replacement using the Phaser tool of PHENIX software package (https://phenix-online.org/) and two ensembles as search model: one corresponding to R0RB:pUb from structure of human pUbl-R0RB:pUb (PDB 6GLC) and a second corresponding to pUb alone. Refinements were performed with PHENIX (48), and model building was performed with COOT (49).

ITC

ITC measurements were carried out using VP-ITC (Microcal) at 20 °C in 50 mM Tris, 150 mM NaCl, 1 mM TCEP, pH 7.4 with parkin R0RB or a one-to-one complex of R0RB–pUb in the cell titrated with one injection of 5 μl followed by 28 injections of 10 μl of either pUbl or pUbl-ACT. Results were analyzed using ORIGIN v7 software (MicroCal) and fitted to a single site-binding model.

Data availability

The atomic coordinates and structure factors (accession code 7US1) have been deposited in the Protein Data Bank.

Supporting information—This article contains supporting information.

Acknowledgments—The authors thank Drs Simon Veyron and Guennadi Kozlov for assistance with the crystal structure data processing and refinement. This work was supported by Michael J. Fox Foundation grant (MJFF-019029) and Canadian Institutes of Health Research grant (FDN 159903).

Author contributions—R. F., V. S., and K. G. methodology; R. F. and V. S. investigation; V. S. and R. F. data curation; R. F., V. S, and K. G. writing–original draft.

Conflict of interest—The authors declare that they have no conflicts of interest with the contents of this article.

Abbreviations—The abbreviations used are: ACT, activation; ITC, isothermal titration calorimetry; PD, Parkinson's disease; pUb, phosphorylated ubiquitin; TCEP, tris(2-carboxyethyl)phosphine; Ubl, ubiquitin-like domain.

References

1. Koros, C., Simitsi, A., and Stefanis, L. (2017) Genetics of Parkinson's disease: genotype-phenotype correlations. *Int. Rev. Neurobiol.* **132**, 197–231

2. Kitada, T., Asakawa, S., Hattori, N., Matsumine, H., Yamamura, Y., Minoshima, S., *et al.* (1998) Mutations in the parkin gene cause autosomal recessive juvenile parkinsonism. *Nature* **392**, 605–608
3. Valente, E. M., Abou-Sleiman, P. M., Caputo, V., Muqit, M. M., Harvey, K., Gispert, S., *et al.* (2004) Hereditary early-onset Parkinson's disease caused by mutations in PINK1. *Science* **304**, 1158–1160
4. Pickles, S., Vigie, P., and Youle, R. J. (2018) Mitophagy and quality control mechanisms in mitochondrial maintenance. *Curr. Biol.* **28**, R170–R185
5. Sugiura, A., McLelland, G. L., Fon, E. A., and McBride, H. M. (2014) A new pathway for mitochondrial quality control: mitochondrial-derived vesicles. *EMBO J.* **33**, 2142–2156
6. Matheoud, D., Sugiura, A., Bellemare-Pelletier, A., Laplante, A., Rondeau, C., Chemali, M., *et al.* (2016) Parkinson's disease-related proteins PINK1 and parkin repress mitochondrial antigen presentation. *Cell* **166**, 314–327
7. Wenzel, D. M., Lissounov, A., Brzovic, P. S., and Klevit, R. E. (2011) UBCH7 reactivity profile reveals parkin and HHARI to be RING/HECT hybrids. *Nature* **474**, 105–108
8. Riley, B. E., Lougheed, J. C., Callaway, K., Velasquez, M., Brecht, E., Nguyen, L., *et al.* (2013) Structure and function of Parkin E3 ubiquitin ligase reveals aspects of RING and HECT ligases. *Nat. Commun.* **4**, 1982
9. Trempe, J. F., Sauve, V., Grenier, K., Seirafi, M., Tang, M. Y., Menade, M., *et al.* (2013) Structure of parkin reveals mechanisms for ubiquitin ligase activation. *Science* **340**, 1451–1455
10. Wauer, T., and Komander, D. (2013) Structure of the human parkin ligase domain in an autoinhibited state. *EMBO J.* **32**, 2099–2112
11. Geisler, S., Holmstrom, K. M., Skujat, D., Fiesel, F. C., Rothfuss, O. C., Kahle, P. J., *et al.* (2010) PINK1/parkin-mediated mitophagy is dependent on VDAC1 and p62/SQSTM1. *Nat. Cell Biol.* **12**, 119–131
12. Matsuda, N., Sato, S., Shiba, K., Okatsu, K., Saisho, K., Gautier, C. A., *et al.* (2010) PINK1 stabilized by mitochondrial depolarization recruits parkin to damaged mitochondria and activates latent parkin for mitophagy. *J. Cell Biol.* **189**, 211–221
13. Narendra, D. P., Jin, S. M., Tanaka, A., Suen, D. F., Gautier, C. A., Shen, J., *et al.* (2010) PINK1 is selectively stabilized on impaired mitochondria to activate parkin. *PLoS Biol.* **8**, e1000298
14. Vives-Bauza, C., Zhou, C., Huang, Y., Cui, M., de Vries, R. L., Kim, J., *et al.* (2010) PINK1-dependent recruitment of parkin to mitochondria in mitophagy. *Proc. Natl. Acad. Sci. U. S. A.* **107**, 378–383
15. Kane, L. A., Lazarou, M., Fogel, A. I., Li, Y., Yamano, K., Sarraf, S. A., *et al.* (2014) PINK1 phosphorylates ubiquitin to activate parkin E3 ubiquitin ligase activity. *J. Cell Biol.* **205**, 143–153
16. Kazlauskaite, A., Kondapalli, C., Gourlay, R., Campbell, D. G., Ritorto, M. S., Hofmann, K., *et al.* (2014) Parkin is activated by PINK1-dependent phosphorylation of ubiquitin at Ser65. *Biochem. J.* **460**, 127–139
17. Sauve, V., Lilov, A., Seirafi, M., Vranas, M., Rasool, S., Kozlov, G., *et al.* (2015) A Ubl/ubiquitin switch in the activation of parkin. *EMBO J.* **34**, 2492–2505
18. Wauer, T., Simicek, M., Schubert, A., and Komander, D. (2015) Mechanism of phospho-ubiquitin-induced PARKIN activation. *Nature* **524**, 370–374
19. Koyano, F., Okatsu, K., Kosako, H., Tamura, Y., Go, E., Kimura, M., *et al.* (2014) Ubiquitin is phosphorylated by PINK1 to activate parkin. *Nature* **510**, 162–166
20. Ordureau, A., Sarraf, S. A., Duda, D. M., Heo, J. M., Jedrychowski, M. P., Sviderskiy, V. O., *et al.* (2014) Quantitative proteomics reveal a feedforward mechanism for mitochondrial PARKIN translocation and ubiquitin chain synthesis. *Mol. Cell* **56**, 360–375
21. Kazlauskaite, A., Martinez-Torres, R. J., Wilkie, S., Kumar, A., Peltier, J., Gonzalez, A., *et al.* (2015) Binding to serine 65-phosphorylated ubiquitin primes parkin for optimal PINK1-dependent phosphorylation and activation. *EMBO Rep.* **16**, 939–954
22. Kondapalli, C., Kazlauskaite, A., Zhang, N., Woodroof, H. I., Campbell, D. G., Gourlay, R., *et al.* (2012) PINK1 is activated by mitochondrial membrane potential depolarization and stimulates parkin E3 ligase activity by phosphorylating serine 65. *Open Biol.* **2**, 120080
23. Kumar, A., Aguirre, J. D., Condos, T. E., Martinez-Torres, R. J., Chaugule, V. K., Toth, R., *et al.* (2015) Disruption of the autoinhibited state primes the E3 ligase parkin for activation and catalysis. *EMBO J.* **34**, 2506–2521
24. Wauer, T., Swatek, K. N., Wagstaff, J. L., Gladkova, C., Pruneda, J. N., Michel, M. A., *et al.* (2015) Ubiquitin Ser65 phosphorylation affects ubiquitin structure, chain assembly and hydrolysis. *EMBO J.* **34**, 307–325
25. Kumar, A., Chaugule, V. K., Condos, T. E. C., Barber, K. R., Johnson, C., Toth, R., *et al.* (2017) Parkin-phosphoubiquitin complex reveals cryptic ubiquitin-binding site required for RBR ligase activity. *Nat. Struct. Mol. Biol.* **24**, 475–483
26. Sauve, V., Sung, G., Soya, N., Kozlov, G., Blaimschein, N., Miotto, L. S., *et al.* (2018) Mechanism of parkin activation by phosphorylation. *Nat. Struct. Mol. Biol.* **25**, 623–630
27. Gladkova, C., Maslen, S. L., Skehel, J. M., and Komander, D. (2018) Mechanism of parkin activation by PINK1. *Nature* **559**, 410–414
28. Seirafi, M., Kozlov, G., and Gehring, K. (2015) Parkin structure and function. *FEBS J.* **282**, 2076–2088
29. Lazarou, M., Narendra, D. P., Jin, S. M., Tekle, E., Banerjee, S., and Youle, R. J. (2013) PINK1 drives parkin self-association and HECT-like E3 activity upstream of mitochondrial binding. *J. Cell Biol.* **200**, 163–172
30. Shiba-Fukushima, K., Arano, T., Matsumoto, G., Inoshita, T., Yoshida, S., Ishihama, Y., *et al.* (2014) Phosphorylation of mitochondrial polyubiquitin by PINK1 promotes parkin mitochondrial tethering. *PLoS Genet.* **10**, e1004861
31. Sauvé, V., Sung, G., MacDougall, E. J., Kozlov, G., Saran, A., Fakih, R., *et al.* (2022) Structural basis for feedforward control in the PINK1/parkin pathway. *EMBO J.* **41**, e109460
32. Shiba-Fukushima, K., Imai, Y., Yoshida, S., Ishihama, Y., Kanao, T., Sato, S., *et al.* (2012) PINK1-mediated phosphorylation of the parkin ubiquitin-like domain primes mitochondrial translocation of parkin and regulates mitophagy. *Sci. Rep.* **2**, 1002
33. Tang, M. Y., Vranas, M., Krahn, A. I., Pundlik, S., Trempe, J. F., and Fon, E. A. (2017) Structure-guided mutagenesis reveals a hierarchical mechanism of parkin activation. *Nat. Commun.* **8**, 14697
34. Zhuang, N., Li, L., Chen, S., and Wang, T. (2016) PINK1-dependent phosphorylation of PINK1 and parkin is essential for mitochondrial quality control. *Cell Death Dis.* **7**, e2501
35. Yi, W., MacDougall, E. J., Tang, M. Y., Krahn, A. I., Gan-Or, Z., Trempe, J. F., *et al.* (2019) The landscape of parkin variants reveals pathogenic mechanisms and therapeutic targets in Parkinson's disease. *Hum. Mol. Genet.* **28**, 2811–2825
36. Wu, R. M., Bounds, R., Lincoln, S., Hulihan, M., Lin, C. H., Hwu, W. L., *et al.* (2005) Parkin mutations and early-onset parkinsonism in a Taiwanese cohort. *Arch. Neurol.* **62**, 82–87
37. Wang, T., Liang, Z., Sun, S., Cao, X., Peng, H., Cao, F., *et al.* (2003) Point mutation in the parkin gene on patients with Parkinson's disease. *J. Huazhong Univ. Sci. Technol. Med. Sci.* **23**, 145–147
38. Terreni, L., Calabrese, E., Calella, A. M., Forloni, G., and Mariani, C. (2001) New mutation (R42P) of the parkin gene in the ubiquitinlike domain associated with parkinsonism. *Neurology* **56**, 463–466
39. Hoenicka, J., Vidal, L., Morales, B., Ampuero, I., Jiménez-Jiménez, F. J., Berciano, J., *et al.* (2002) Molecular findings in familial Parkinson disease in Spain. *Arch. Neurol.* **59**, 966–970
40. Safadi, S. S., and Shaw, G. S. (2007) A disease state mutation unfolds the parkin ubiquitin-like domain. *Biochemistry* **46**, 14162–14169
41. Trempe, J. F., Chen, C. X., Grenier, K., Camacho, E. M., Kozlov, G., McPherson, P. S., *et al.* (2009) SH3 domains from a subset of BAR proteins define a Ubl-binding domain and implicate parkin in synaptic ubiquitination. *Mol. Cell* **36**, 1034–1047
42. Stuber, K., Schneider, T., Werner, J., Kovermann, M., Marx, A., and Scheffner, M. (2021) Structural and functional consequences of NEDD8 phosphorylation. *Nat. Commun.* **12**, 5939
43. Balasubramaniam, M., Parcon, P. A., Bose, C., Liu, L., Jones, R. A., Farlow, M. R., *et al.* (2019) Interleukin-1beta drives NEDD8 nuclear-to-cytoplasmic translocation, fostering parkin activation via NEDD8 binding to the P-ubiquitin activating site. *J. Neuroinflammation* **16**, 275

44. Schuck, P. (2004) A model for sedimentation in inhomogeneous media. I. Dynamic density gradients from sedimenting co-solutes. *Biophys. Chem.* **108**, 187–200
45. Brautigam, C. A. (2015) Calculations and publication-quality illustrations for analytical ultracentrifugation data. *Methods Enzymol.* **562**, 109–133
46. Fodje, M., Janzen, K., Berg, R., Black, G., Labiuk, S., Gorin, J., *et al.* (2012) MxDC and MxLIVE: software for data acquisition, information management and remote access to macromolecular crystallography beamlines. *J. Synchrotron Radiat.* **19**, 274–280
47. Kabsch, W. (2010) XDS. *Acta Crystallogr. D Biol. Crystallogr.* **66**, 125–132
48. Adams, P. D., Afonine, P. V., Bunkoczi, G., Chen, V. B., Davis, I. W., Echols, N., *et al.* (2010) PHENIX: a comprehensive python-based system for macromolecular structure solution. *Acta Crystallogr. D Biol. Crystallogr.* **66**, 213–221
49. Emsley, P., Lohkamp, B., Scott, W. G., and Cowtan, K. (2010) Features and development of Coot. *Acta Crystallogr. D Biol. Crystallogr.* **66**, 486–501